

# Enhancement of CA3 hippocampal network activity by activation of group II metabotropic glutamate receptors

Jeanne Ster<sup>a</sup>, José María Mateos<sup>a,b</sup>, Benjamin Friedrich Grewe<sup>a</sup>, Guylleume Coiret<sup>a</sup>, Corrado Corti<sup>c,1</sup>, Mauro Corsi<sup>c,1</sup>, Fritjof Helmchen<sup>a</sup>, and Urs Gerber<sup>a,2</sup>

<sup>a</sup>Brain Research Institute, University of Zurich, CH-8057 Zurich, Switzerland; <sup>b</sup>Center for Microscopy and Image Analysis, University of Zurich, CH-8057 Zurich, Switzerland; and <sup>c</sup>Department of Biology, Neuroscience Centre of Excellence in Drug Discovery, GlaxoSmithKline Medicines Research Centre, 37135 Verona, Italy

Edited by Floyd Bloom, The Scripps Research Institute, La Jolla, CA, and approved May 11, 2011 (received for review January 12, 2011)

**Impaired function or expression of group II metabotropic glutamate receptors (mGluRIs) is observed in brain disorders such as schizophrenia. This class of receptor is thought to modulate activity of neuronal circuits primarily by inhibiting neurotransmitter release. Here, we characterize a postsynaptic excitatory response mediated by somato-dendritic mGluRIs in hippocampal CA3 pyramidal cells and in stratum oriens interneurons. The specific mGluRII agonists DCG-IV or LCCG-1 induced an inward current blocked by the mGluRII antagonist LY341495. Experiments with transgenic mice revealed a significant reduction of the inward current in mGluR3<sup>-/-</sup> but not in mGluR2<sup>-/-</sup> mice. The excitatory response was associated with periods of synchronized activity at theta frequency. Furthermore, cholinergically induced network oscillations exhibited decreased frequency when mGluRIs were blocked. Thus, our data indicate that hippocampal responses are modulated not only by presynaptic mGluRIs that reduce glutamate release but also by postsynaptic mGluRIs that depolarize neurons and enhance CA3 network activity.**

The physiological roles in the hippocampus of group II mGluRs (mGluRIIs), comprised of mGluR2 and mGluR3, were first characterized at mossy fiber synapses in the CA3 region, where their activation was shown to inhibit neurotransmitter release (1–4) and to induce long-term depression (5–8). In addition, mGluRIIs modulate GABA release in hippocampal interneurons (9) and in granule cells of the accessory olfactory bulb (10). Apart from their presence in the preterminal zone of mossy fibers (5, 11), mGluRIIs in the hippocampus are also localized in the somato-dendritic region of pyramidal cells (12–14), but their function is unknown. In other brain areas, activation of somatic mGluRIIs reduces calcium currents in cultured cerebellar granule cells (15, 16), in cerebellar Golgi cells (17), and in interneurons of the olfactory bulb (18) and accessory olfactory bulb (17). In contrast, calcium currents are increased in cortical neurons (19).

Agonists for mGluRIIs have shown promise in animal models for stroke, epilepsy, neurodegenerative diseases, schizophrenia, anxiety, and drug addiction (20, 21). In patients with schizophrenia, there is down-regulation of mGluR2 (22) and alterations in mGluR3 (23). Moreover, recent clinical trials showed positive results for mGluRII agonists in reducing symptoms in schizophrenia (24). To improve our understanding of how these receptors modulate neuronal activity, we have characterized responses mediated by postsynaptic mGluRIIs.

## Results

**Activation of mGluRIIs Increases Spontaneous Synaptic Activity in Pyramidal Cells.** As mGluRIIs are not expressed on the associational/commissural fibers in the hippocampal CA3 area, pharmacological stimulation of these receptors on mossy fibers represents a key strategy to distinguish between excitatory synaptic responses originating from dentate granule cells as opposed to CA3 pyramidal cells (25). However, we observed that bath application of

the mGluRII agonists DCG-IV (2  $\mu$ M) or LCCG-1 (10  $\mu$ M) also resulted in a pronounced increase in spontaneous synaptic activity in CA3 pyramidal cells (Fig. 1). Before characterizing this response, we confirmed that these agonists blocked mossy fiber transmission under our experimental conditions. In recordings from monosynaptically connected pairs of granule cells and CA3 pyramidal cells in hippocampal slice cultures (26), application of DCG-IV at 2  $\mu$ M completely blocked synaptic transmission in three of four granule cell–pyramidal cell pairs (98  $\pm$  2%) and induced a partial block in the remaining pair (by 56%), resulting in an 88  $\pm$  10% mean reduction in charge transfer of evoked responses ( $n = 4$ ; Fig. S1). Comparable values were reported in earlier studies using minimal stimulation (27–29). DCG-IV did not reduce evoked responses between synaptically coupled CA3 pyramidal cells (18.7  $\pm$  8%,  $P > 0.87$ ; Fig. S1).

The observed increase in spontaneous synaptic activity suggests that DCG-IV or LCCG-1 induces action potential discharge in CA3 pyramidal cells and interneurons by activating mGluRIIs with a somato-dendritic localization, as was shown in morphological studies. Because many of our experiments were performed in slice cultures, we examined receptor localization by electron microscopy using an anti-mGluR2/3 antibody. We found that, as in acutely studied tissue (12–14), immunoreactivity was present postsynaptically on dendritic spines as well as presynaptically (Fig. 1D and Fig. S1C).

Analysis of the effect of DCG-IV (2  $\mu$ M, 10 min) on spontaneous synaptic events in CA3 pyramidal cells revealed a 5.5-fold increase in the frequency of spontaneous excitatory postsynaptic currents (EPSCs) (654  $\pm$  135%,  $n = 8$ ) and a 23-fold increase in spontaneous inhibitory postsynaptic currents (IPSCs) (2,419  $\pm$  269%,  $n = 8$ ; Fig. 1A and C). The increase in amplitude, which was due to the summation of high-frequency unitary events, was significant for EPSPs (1.9-fold) but not for IPSPs (EPSCs: 286  $\pm$  69%,  $P < 0.004$ ; IPSCs: 290  $\pm$  108%,  $P > 0.1$ ,  $n = 8$ ; Fig. 1A and C). Comparable responses were induced by LCCG-1 (10  $\mu$ M, 10 min), another mGluRII agonist (frequency: 827  $\pm$  287% for EPSCs and 2,335  $\pm$  532% for IPSCs; amplitude: 161  $\pm$  17% for EPSCs and 261  $\pm$  110% for IPSCs;  $n = 7$ ; Fig. 1B and D). The postsynaptic response mediated by mGluRIIs is not peculiar to slice cultures, as this effect of DCG-IV was also induced in acute

Author contributions: J.S. and U.G. designed research; J.S., J.M.M., B.F.G., and G.C. performed research; J.M.M., C.C., M.C., and F.H. contributed new reagents/analytic tools; J.S., B.F.G., F.H., and U.G. analyzed data; and J.S. and U.G. wrote the paper.

The authors declare no conflict of interest.

This article is a PNAS Direct Submission.

<sup>1</sup>Present address: Aptuit Srl., Molecular and Cell Biology, via Fleming 4, 37135 Verona, Italy.

<sup>2</sup>To whom correspondence should be addressed. E-mail: gerber@hifo.uzh.ch.

This article contains supporting information online at [www.pnas.org/lookup/suppl/doi:10.1073/pnas.1100548108/-DCSupplemental](http://www.pnas.org/lookup/suppl/doi:10.1073/pnas.1100548108/-DCSupplemental).

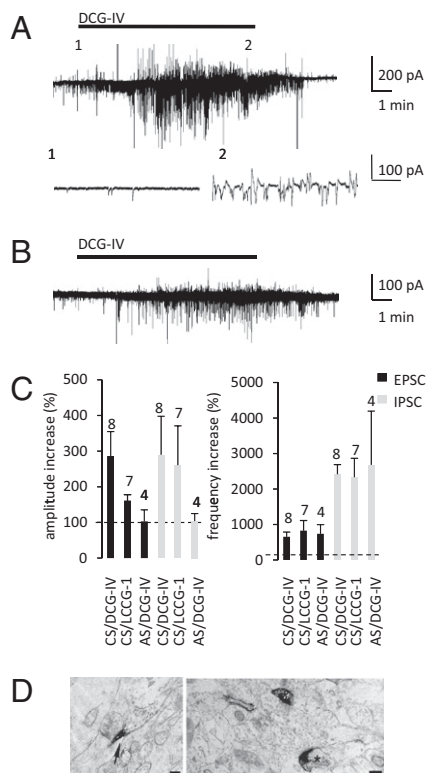


**Fig. 1.** Stimulation of mGluR1s increases synaptic activity recorded from CA3 pyramidal cells in acute as well as in cultured hippocampal slices. (A) DCG-IV (2  $\mu$ M) increases amplitude and frequency of EPSCs and IPSCs in slice culture. (Lower) Expanded traces of spontaneous activity in the absence (1) and in the presence of DCG-IV (2). (B) Effects of DCG-IV in an acute slice. (C) Quantification of spontaneous activity (black: EPSCs; gray: IPSCs) induced by DCG-IV and LCCG-1 in cultured slices (CS) or acute slices (AS). (D) Subcellular localization of mGluR2/3 in the CA3 area of hippocampal slice cultures. mGluR2/3 is expressed in the preterminal region and along the length of axons (arrow). Asterisks indicate postsynaptic mGluR2/3 in dendrites in CA3 neurons. (Scale bars: 0.2  $\mu$ m.)

hippocampal slices (frequency:  $738 \pm 258\%$  for EPSCs and  $2,683 \pm 1515\%$  for IPSCs; amplitude:  $102 \pm 33\%$  for EPSCs,  $104 \pm 21\%$  for IPSCs,  $n = 4$ , Fig. 1C). As the actions of LCCG-1 and DCG-IV on the amplitude and the frequency of spontaneous synaptic events were not significantly different ( $P > 0.06$  for EPSCs and IPSCs, amplitude as well as frequency), either agonist was used in subsequent experiments.

**Activation of mGluR1s Induces Inward Current in CA3 Pyramidal Cells and Interneurons.** We reasoned that the pronounced increase in synaptic activity induced by LCCG-1 or DCG-IV may reflect a depolarization of pyramidal cells and interneurons mediated by the activation of somato-dendritic mGluR1s. Indeed, in slice cultures in the presence of TTX (1  $\mu$ M) and picrotoxin (100  $\mu$ M), CA3 pyramidal cells voltage-clamped at  $-70$  mV responded to DCG-IV (2  $\mu$ M, 10 min; Fig. 2A) or LCCG-1 (10  $\mu$ M) with an inward current of  $-26.4 \pm 4.7$  pA ( $n = 16$ ) or  $-34.9 \pm 4.9$  pA ( $n = 7$ ), respectively. In acute slices, DCG-IV induced an inward current of comparable amplitude ( $-47.0 \pm 14.5$  pA,  $n = 3$ ). The mGluR1 antagonist LY341495 (3  $\mu$ M) blocked DCG-IV-induced inward current to  $-3.5 \pm 1.9$  pA ( $n = 7$ ,  $P < 0.01$ ; Fig. 2B), whereas mGluR antagonists for group I (MPEP and CPCCOEt, Fig. S2) and group III (MSOP, 100  $\mu$ M, Fig. S2), as well as the NMDA receptor antagonist D-AP5 (40  $\mu$ M,  $-14.9 \pm 3.9$  pA; Fig. 2B) had no effect. Interneurons in CA3 stratum oriens responded to DCG-IV (2  $\mu$ M, 10 min) with an inward current of  $-23.9 \pm 5.3$  pA (Fig. S3,

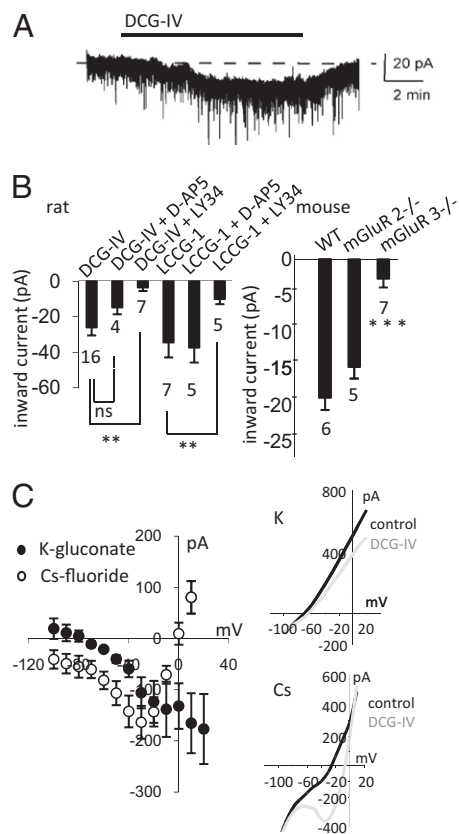


**Fig. 2.** DCG-IV applied to CA3 pyramidal cells induces inward current associated with a decrease in potassium and an increase in cationic conductance. (A) Upper trace shows inward current induced by DCG-IV (2  $\mu$ M, 10 min) in a CA3 pyramidal cell voltage clamped at  $-70$  mV in the presence of TTX and picrotoxin. (B) Quantification of inward current induced by DCG-IV, by DCG-IV in the presence of the group II antagonist LY341495 or an NMDAR antagonist D-AP5, by LCCG-1, and by LCCG-1 in presence of D-AP5 or LY341495 (Left); quantification of inward current induced by DCG-IV in wild type (WT), mGluR2 $^{-/-}$ , and mGluR3 $^{-/-}$  mice (Right). (C) Subtracted I-V relationships (Left) in rat pyramidal cells obtained with voltage steps incrementing by 10-mV steps indicating a reduction in K conductance when measured with a K $^{+}$ -based intracellular medium and (open circles) an increase in a cationic conductance with a Cs $^{+}$ -based intracellular medium ( $n = 6$ ). (Right) Current traces from a representative experiment obtained in the presence of DCG-IV (black line) or in the presence of DCG-IV and CPA (gray line) with a K $^{+}$ -based intracellular medium (Top) or with a Cs $^{+}$ -based intracellular medium (Bottom).

$n = 5$ ). Again, the DCG-IV-induced inward current was blocked by LY341495 (Fig. S3,  $n = 4$ ), but not by D-AP5 (Fig. S3,  $n = 4$ ).

We assessed whether the absence of mGluR2 or of mGluR3 affects the inward current induced by DCG-IV in CA3 pyramidal cells and in CA3 interneurons. In CA3 pyramidal cells, the efficacy of DCG-IV (2  $\mu$ M) was strongly reduced in mGluR3 $^{-/-}$  slice cultures compared with WT cultures (WT =  $-19.0 \pm 1.7$  pA,  $n = 6$ ; mGluR3 $^{-/-}$  =  $-2.7 \pm 1.2$  pA,  $n = 7$ ,  $P < 0.0005$ ,  $n = 5$ ; Fig. 2B). In contrast, there was no significant difference in the induced inward current between mGluR2 $^{-/-}$  and WT (mGluR2 $^{-/-}$  =  $-14.8 \pm 1.7$  pA,  $n = 5$ ; Fig. 2B). This was also the case for interneurons (WT =  $-22.0 \pm 4.5$  pA,  $n = 6$ ; mGluR3 $^{-/-}$  =  $-5.3 \pm 1.9$  pA,  $n = 6$ ; mGluR2 $^{-/-}$  =  $-23.4 \pm 5.4$  pA,  $n = 5$ ; Fig. S3B).

**Inward Currents Are Mediated by Inhibition of K $^{+}$  Conductance and Activation of Cationic Conductance.** We characterized the inward current in CA3 pyramidal cells with a voltage-clamp step protocol using a standard potassium gluconate intracellular medium

(Fig. 2C). The response induced by DCG-IV was associated with a reduced slope of the current–voltage (I/V) relationship. The I/V curves in control and in presence of DCG-IV intersected at  $-77.4 \pm 3$  mV (Fig. 2C,  $n = 6$ ). This reversal potential is close to the equilibrium potential for potassium ( $V_m = -100$  mV), with the positive shift probably indicating a contribution from a cationic conductance. Indeed, with a cesium-based intracellular solution to block most potassium channels, DCG-IV increased the slope of the I/V relationship, yielding a reversal potential of  $1 \pm 2.7$  mV ( $n = 6$ , Fig. 2C). Moreover, this current was voltage-dependent, being maximal at  $-35$  mV and declining at more hyperpolarized voltages, suggesting that activated channels were sensitive to intracellular calcium concentration. We therefore recorded intracellular calcium levels by injecting the calcium dye OGB1-AM locally into slice cultures through a patch pipette. At the end of experiments, sulforhodamine 101 ( $1 \mu\text{M}$ ) was applied for 5 min to distinguish astrocytes (30). Optical imaging of CA3 pyramidal cells showed evoked calcium signals in 90.9% of the cells in response to LCCG-1 application ( $n = 22$  in 2 slices). In many cases, rapid calcium transients likely triggered by action potentials (APs) were observed (Fig. 3A). Accordingly, application of LCCG-1 ( $10 \mu\text{M}$ , 10 min) induced action potential firing in CA3 pyramidal cells ( $n = 5/5$ , Fig. 3B). When LCCG-1 was applied in the presence of TTX, sharp calcium transients were abolished but the somatic calcium elevation was maintained in 92% of neurons ( $16.2 \pm 0.2\%$ , mean  $\Delta F/F$  calculated over 1 min after 5 min of LCCG-1 application;  $n = 69$ , 5 slices; Fig. 3C and

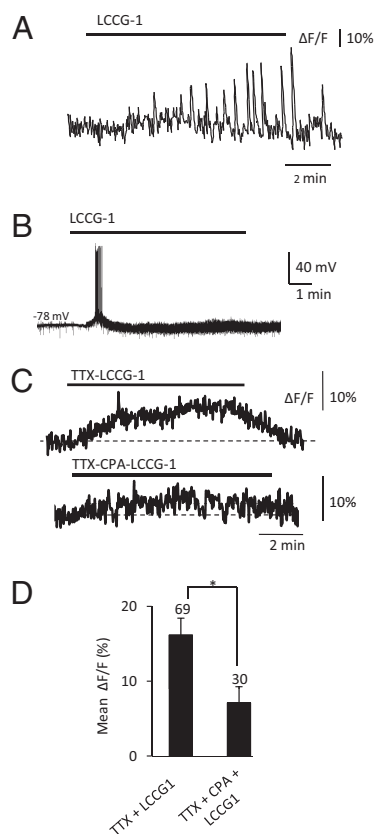


**Fig. 3.** Calcium responses mediated by mGluRIIs. (A) A barrage of calcium transients evoked by LCCG-1 in a CA3 pyramidal cell. (B) In current clamp mode, LCCG-1 induces a depolarization resulting in action potential firing, accompanied by an increase in synaptic noise. (C) Addition of TTX blocks calcium spikes but not the maintained calcium rise induced by LCCG-1. Emptying calcium stores with CPA reduces the calcium rise. (D) Histogram represents the mean  $\Delta F/F$  (%) to illustrate the effect of CPA.

D). The calcium elevation in TTX was reduced significantly when calcium stores were depleted following treatment with cyclopiiazonic acid (CPA), a  $\text{Ca}^{2+}$ -ATPase inhibitor ( $7.1 \pm 2.2\%$ ,  $n = 30$ , 3 slices; Fig. 3C and D). The means of the  $\Delta F/F$  in the presence of TTX and in the presence of TTX + CPA were not significantly different (TTX =  $0.1 \pm 0.2$ , TTX + CPA =  $-0.2 \pm 0.1$ ,  $P > 0.06$ ). CPA also significantly reduced the inward current mediated by mGluRIIs (DCG-IV  $2 \mu\text{M}$ :  $159.7 \pm 29.8$  pA in control,  $71 \pm 24$  pA in CPA, at  $V_{\text{hold}} -10$  mV,  $P = 0.03$ ,  $n = 9$ ; Fig. S4). Thus, the increase in intracellular calcium levels mediated by mGluRIIs facilitates the induction of a cationic inward-current.

#### Synchronous Network Activity in CA3 Induced by mGluRII Activation.

To determine whether the increase in neuronal excitability affects hippocampal network activity, we recorded simultaneously from pairs of unconnected CA3 pyramidal cells in slice cultures. Bath application of LCCG-1 synchronized spontaneous synaptic responses [Fig. 4A;  $n = 4$ , cross-correlation function (CCF) =  $0.7 \pm 0.1$ ]. Moreover, auto-correlograms indicated that the synaptic activity was rhythmic in the theta range ( $13.3 \pm 2.0$  Hz,  $n = 7$ ). D-AP5 has no effect on LCCG-1-induced rhythmic activity ( $14.2 \pm 0.7$  Hz,  $n = 5$ ). The synchronous activity was no longer present 10 min after washout of agonist and was never observed

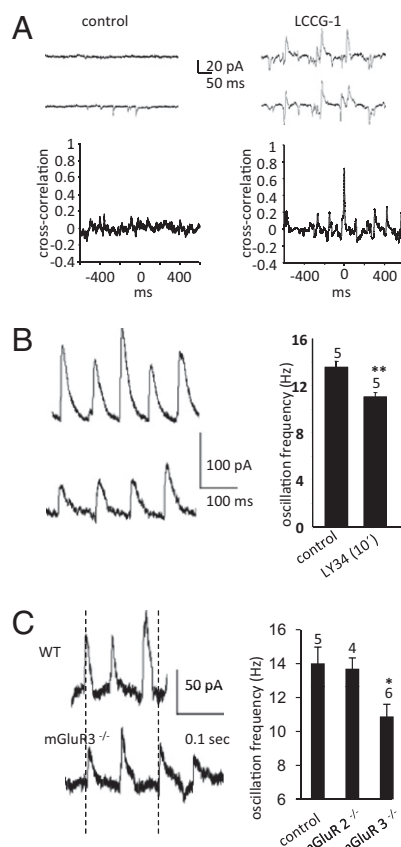


**Fig. 4.** Activating mGluRIIs synchronizes network activity. (A) (Upper) LCCG1 ( $10 \mu\text{M}$ , 10 min) in rat slice cultures increases synaptic activity in two unconnected pyramidal cells leading to synchronized synaptic events. (Lower) Cross-correlograms of spontaneous synaptic activity in the two cells during control (Left) and in the presence of LCCG-1 (Right). (B) Methacholine ( $500$  nM) induces oscillations that are significantly decreased by the group II mGluR antagonist LY341495 ( $n = 5$ ). (C) LCCG1 ( $10 \mu\text{M}$ , 10 min) induces oscillations of the same frequency in wild type (WT) and in  $\text{mGluR}2^{-/-}$ , but at lower frequency in  $\text{mGluR}3^{-/-}$  mice.

in the absence of LCCG-1 ( $n = 4$ ). Rhythmic activity was abolished after blocking AMPA/kainate receptors with NBQX (20  $\mu\text{M}$ ) or by preventing action potential firing with TTX ( $n = 15$ ), indicating that synchronization is a network property. Bath application of methacholine (500 nM, 30 min) induced rhythmic oscillations in slice cultures (31), which commenced within 4–5 min after onset and peaked after 20 min ( $13.5 \pm 0.3$  Hz,  $n = 5$ ; Fig. 4B). The frequency of oscillations was significantly reduced in the presence of the mGluRII antagonist LY341495 (3  $\mu\text{M}$ ) to  $11.1 \pm 0.5$  Hz ( $n = 5$ ,  $P < 0.004$ , Fig. 4B), indicating that mGluRIIs contribute to the generation of hippocampal theta oscillations. Experiments were then performed in mice to determine the contribution of mGluR2 and mGluR3 to the oscillatory response. The frequency of oscillations induced by LCCG-1 (10  $\mu\text{M}$ , 10 min) was  $14.0 \pm 1.0$  Hz in WT and  $13.7 \pm 0.6$  Hz in mGluR2<sup>-/-</sup>, which is not significantly different ( $P > 0.05$ ). In contrast, LCCG-1 induced oscillations of significantly lower frequency in mGluR3<sup>-/-</sup> mice ( $10.9 \pm 0.7$  Hz;  $P < 0.05$ ; Fig. 4C). Thus, mGluRIIs, most likely in conjunction with other G protein-coupled receptors, can contribute to the entrainment of hippocampal network activity in the theta range.

## Discussion

We have shown that activation of group II mGluRs enhances hippocampal network activity by depolarizing neurons and thus increasing excitability in the CA3 area. At the same time, these receptors mediate inhibition of mossy fiber transmission, as previously characterized (1–4). This neuronal excitation is consistent with the previously described expression of mGluRIIs in the somato-dendritic compartment of hippocampal neurons (12–14). As mGluRII agonists block mossy fiber transmission, the main source of the EPSCs was input from neighboring CA3 pyramidal cells. Characterization of the inward current mediated by somato-dendritic mGluRIIs indicated three underlying processes including release of intracellular calcium stores, activation of a calcium-sensitive cationic conductance, and inhibition of a potassium conductance (Figs. 2 and 3). Our experiments with knockout mice identified mGluR3 as the receptor responsible for the inward current, consistent with previous studies showing that reduction of synaptic transmission involves primarily mGluR2 (5, 32) whereas mGluR3 exhibits predominantly a postsynaptic dendritic localization (14, 32). We also noted a differential effect mediated by mGluR2 and mGluR3 in the induction of oscillatory activity. Oscillatory activity represents an intrinsic mode of hippocampal function emerging as a consequence of specific dendritic conductances and the configuration of synaptic circuits. The switch into the oscillatory mode can be triggered by a variety of neurotransmitters such as acetylcholine and glutamate that activate inhibitory interneurons, which pace oscillations and principal cells (33). A similar mechanism is likely to come into play following the activation of mGluRII receptors. In the case of mGluR3<sup>-/-</sup> mice, only a small inward current was induced by mGluRII agonists, which may explain the lower frequency of oscillations observed in mGluR3<sup>-/-</sup> compared with WT or mGluR2<sup>-/-</sup> mice (Fig. 4).

The finding that mGluRIIs can act as axonal autoreceptors to inhibit vesicular glutamate release led to the proposal that specific agonists should be useful in treating diseases associated with excessive extracellular glutamate levels. Indeed, mGluRII agonists have been shown to reduce excitotoxicity in animal models of brain disorders (20). However, in the case of a multifactorial

illness such as schizophrenia, the efficacy of treatment with an mGluRII agonist (24) is likely to involve additional mechanisms. Our results suggest that the therapeutic actions of mGluRII agonists are based not only on their actions at autoreceptors but also on their ability to modulate network rhythmicity. Indeed, accruing evidence indicates that the uncoordinated cognitive processing underlying many of the symptoms in schizophrenia is related to abnormal theta and gamma oscillations (34). Interestingly, activation of group I mGluRs also induces network oscillations (35, 36). Furthermore, the conditions under which somatic mGluRIIs are activated should lead to concomitant activation of group I mGluRs, allowing these two classes of receptor to operate synergistically in the regulation of rhythmic discharge. Because the enhancement of network activity in the CA3 region is associated with mGluRII-mediated inhibition of input arriving via the mossy fibers and the perforant path, this functional reconfiguration of the circuitry may shield the CA3 network from extraneous input during the critical period when memory traces undergo stabilization (37).

## Materials and Methods

Hippocampal slice cultures were prepared from 6-d-old rat pups killed by decapitation and maintained for 3–5 wk in vitro (38). Hippocampal acute slices (400  $\mu\text{m}$ ) were prepared from 14- to 21-d-old Wistar rats. Acute slices or slice cultures were then transferred to a submerged recording chamber mounted on an upright microscope (Axioskop FS1, Zeiss) and superfused with artificial cerebrospinal fluid (ACSF) for acute slices or an external solution containing (mM) 137 NaCl, 2.7 KCl, 11.6 NaHCO<sub>3</sub>, 0.4 NaH<sub>2</sub>PO<sub>4</sub>, 2 MgCl<sub>2</sub>, 3 CaCl<sub>2</sub>, 5.6 D-glucose, and 0.001% phenol red for slice cultures. All experiments were performed at 33 °C.

Whole-cell recordings of CA3 pyramidal cells and dentate granule cells were obtained with patch pipettes (4–6 M $\Omega$ ). Pipettes were filled either with (mM) 135 K-gluconate, 5 KCl, 10 Hepes, 1 EGTA, 5 phosphocreatine (CrP), 2 MgATP, 0.4 NaGTP, and 0.07 CaCl<sub>2</sub> or with 125 CsCl, 10 Hepes, 1 EGTA, 5 CrP, 2 MgATP, and 0.4 NaGTP (pH 7.2). For paired recording between granule cells and CA3 pyramidal cells, pyramidal cell pipettes were filled with (mM) 121.6 CsF, 8.4 CsCl, 10 Hepes, 10 EGTA, 1 picrotoxin, 2 MgATP, 5 CrP, and 0.4 NaGTP (pH 7.2). Membrane potentials were corrected for junction potentials. For the determination of current–voltage relationships, command potentials had a duration of 1 s to ensure steady-state responses. Data were recorded with an Axopatch 200B amplifier (Axon Instruments), digitized at 2–5 kHz and analyzed off-line. Autocorrelation and cross-correlation functions were calculated using clampfit (Molecular Devices). One-minute segments were analyzed after 5 min of application of LCCG1. Records were examined by eye, periods of oscillatory activity were chosen by eye, and calculations were performed from the time of the second peak in the autocorrelation function (period). A segment was considered “rhythmic” when the second peak of the autocorrelation function was at least 0.3 and several regularly spaced peaks appeared. Cells were classified as rhythmic when at least 10 rhythmic segments could be identified during the 1-min time period.

Details for electron microscopy and calcium imaging of hippocampal slice cultures are provided in *SI Materials and Methods*. All numerical data are means  $\pm$  SEM. Significance was determined using the *t* test. A smooth line fit was used to generate the curves for the I/V relation (Fig. 2C).

DCG-IV, LCCG-1, EGLU, MSOP, and LY-341495 were purchased from Tocris Cookson. MPEP, PCCOEt, TTX, NBQX, D-AP5, and CPA were purchased from Ascent Scientific. Picrotoxin and sulforhodamine 101 were purchased from Sigma-Aldrich.

**ACKNOWLEDGMENTS.** We thank D. Göckeritz-Dujmovic, L. Spassova, H. Kasper, S. Giger, and R. Schöb for their assistance. We are grateful to Shigetada Nakanishi for permission to use the mGluR2<sup>-/-</sup> mice. We also thank Beat Gähwiler for critically reading the manuscript. This work was funded by the Swiss National Science Foundation.

- Manzoni OJ, Castillo PE, Nicoll RA (1995) Pharmacology of metabotropic glutamate receptors at the mossy fiber synapses of the guinea pig hippocampus. *Neuropharmacology* 34:965–971.
- Scanziani M, Salin PA, Vogt KE, Malenka RC, Nicoll RA (1997) Use-dependent increases in glutamate concentration activate presynaptic metabotropic glutamate receptors. *Nature* 385:630–634.

- Kamiya H, Shinozaki H, Yamamoto C (1996) Activation of metabotropic glutamate receptor type 2/3 suppresses transmission at rat hippocampal mossy fibre synapses. *J Physiol* 493:447–455.
- Capogna M (2004) Distinct properties of presynaptic group II and III metabotropic glutamate receptor-mediated inhibition of perforant pathway-CA1 EPSCs. *Eur J Neurosci* 19:2847–2858.

5. Yokoi M, et al. (1996) Impairment of hippocampal mossy fiber LTD in mice lacking mGluR2. *Science* 273:645–647.
6. Kobayashi K, Manabe T, Takahashi T (1996) Presynaptic long-term depression at the hippocampal mossy fiber-CA3 synapse. *Science* 273:648–650.
7. Huang LQ, Rowan MJ, Anwyl R (1997) mGluR II agonist inhibition of LTP induction, and mGluR II antagonist inhibition of LTD induction, in the dentate gyrus in vitro. *Neuroreport* 8:687–693.
8. Manahan-Vaughan D (1997) Group 1 and 2 metabotropic glutamate receptors play differential roles in hippocampal long-term depression and long-term potentiation in freely moving rats. *J Neurosci* 17:3303–3311.
9. Poncer JC, Shinozaki H, Miles R (1995) Dual modulation of synaptic inhibition by distinct metabotropic glutamate receptors in the rat hippocampus. *J Physiol* 485: 121–134.
10. Hayashi Y, et al. (1993) Role of a metabotropic glutamate receptor in synaptic modulation in the accessory olfactory bulb. *Nature* 366:687–690.
11. Shigemoto R, et al. (1997) Differential presynaptic localization of metabotropic glutamate receptor subtypes in the rat hippocampus. *J Neurosci* 17:7503–7522.
12. Petralia RS, Wang YX, Niedzielski AS, Wenthold RJ (1996) The metabotropic glutamate receptors, mGluR2 and mGluR3, show unique postsynaptic, presynaptic and glial localizations. *Neuroscience* 71:949–976.
13. Neki A, et al. (1996) Pre- and postsynaptic localization of a metabotropic glutamate receptor, mGluR2, in the rat brain: An immunohistochemical study with a monoclonal antibody. *Neurosci Lett* 202:197–200.
14. Tamaru Y, Nomura S, Mizuno N, Shigemoto R (2001) Distribution of metabotropic glutamate receptor mGluR3 in the mouse CNS: Differential location relative to pre- and postsynaptic sites. *Neuroscience* 106:481–503.
15. Chavis P, Shinozaki H, Bockaert J, Fagni L (1994) The metabotropic glutamate receptor types 2/3 inhibit L-type calcium channels via a pertussis toxin-sensitive G-protein in cultured cerebellar granule cells. *J Neurosci* 14:7067–7076.
16. Chavis P, Fagni L, Bockaert J, Lansman JB (1995) Modulation of calcium channels by metabotropic glutamate receptors in cerebellar granule cells. *Neuropharmacology* 34:929–937.
17. Knoflach F, Kemp JA (1998) Metabotropic glutamate group II receptors activate a G protein-coupled inwardly rectifying K<sup>+</sup> current in neurones of the rat cerebellum. *J Physiol* 509:347–354.
18. Bischofberger J, Schild D (1996) Glutamate and N-acetylaspartylglutamate block HVA calcium currents in frog olfactory bulb interneurons via an mGluR2/3-like receptor. *J Neurophysiol* 76:2089–2092.
19. Sugiyama C, et al. (2007) Activator protein-1 responsive to the group II metabotropic glutamate receptor subtype in association with intracellular calcium in cultured rat cortical neurons. *Neurochem Int* 51:467–475.
20. Imre G (2007) The preclinical properties of a novel group II metabotropic glutamate receptor agonist LY379268. *CNS Drug Rev* 13:444–464.
21. Morishima Y, et al. (2005) Enhanced cocaine responsiveness and impaired motor coordination in metabotropic glutamate receptor subtype 2 knockout mice. *Proc Natl Acad Sci USA* 102:4170–4175.
22. González-Maeso J, et al. (2008) Identification of a serotonin/glutamate receptor complex implicated in psychosis. *Nature* 452:93–97.
23. Corti C, et al. (2007) Altered dimerization of metabotropic glutamate receptor 3 in schizophrenia. *Biol Psychiatry* 62:747–755.
24. Patil ST, et al. (2007) Activation of mGlu2/3 receptors as a new approach to treat schizophrenia: A randomized phase 2 clinical trial. *Nat Med* 13:1102–1107.
25. Nicoll RA, Schmitz D (2005) Synaptic plasticity at hippocampal mossy fibre synapses. *Nat Rev Neurosci* 6:863–876.
26. Mori M, Abegg MH, Gähwiler BH, Gerber U (2004) A frequency-dependent switch from inhibition to excitation in a hippocampal unitary circuit. *Nature* 431:453–456.
27. Kwon HB, Castillo PE (2008) Role of glutamate autoreceptors at hippocampal mossy fiber synapses. *Neuron* 60:1082–1094.
28. Rebola N, Lujan R, Cunha RA, Mulle C (2008) Adenosine A2A receptors are essential for long-term potentiation of NMDA-EPSCs at hippocampal mossy fiber synapses. *Neuron* 57:121–134.
29. Toth K, Soares G, Lawrence JJ, Philips-Tansey E, McBain CJ (2000) Differential mechanisms of transmission at three types of mossy fiber synapse. *J Neurosci* 20: 8279–8289.
30. Nimmerjahn A, Kirchhoff F, Kerr JN, Helmchen F (2004) Sulforhodamine 101 as a specific marker of astroglia in the neocortex in vivo. *Nat Methods* 1:31–37.
31. Fischer Y, Wittner L, Freund TF, Gähwiler BH (2002) Simultaneous activation of gamma and theta network oscillations in rat hippocampal slice cultures. *J Physiol* 539: 857–868.
32. Kew JN, Pflimlin MC, Kemp JA, Mutel V (2002) Differential regulation of synaptic transmission by mGlu2 and mGlu3 at the perforant path inputs to the dentate gyrus and CA1 revealed in mGlu2<sup>-/-</sup> mice. *Neuropharmacology* 43:215–221.
33. Buzsáki G (2002) Theta oscillations in the hippocampus. *Neuron* 33:325–340.
34. Ford JM, Krystal JH, Mathalon DH (2007) Neural synchrony in schizophrenia: From networks to new treatments. *Schizophr Bull* 33:848–852.
35. Gillies MJ, et al. (2002) A model of atropine-resistant theta oscillations in rat hippocampal area CA1. *J Physiol* 543:779–793.
36. Pálhalmi J, Paulsen O, Freund TF, Hájos N (2004) Distinct properties of carbachol- and DHPG-induced network oscillations in hippocampal slices. *Neuropharmacology* 47: 381–389.
37. Lynch G, Rex CS, Gall CM (2007) LTP consolidation: Substrates, explanatory power, and functional significance. *Neuropharmacology* 52:12–23.
38. Gähwiler BH (1981) Organotypic monolayer cultures of nervous tissue. *J Neurosci Methods* 4:329–342.